Estimating Total Alkalinity in the Washington State Coastal Zone: Complexities and Surprising Utility for Ocean Acidification Research

Andrea J. Fassbender[*,1], Simone R. Alin[1], Richard A. Feely[1], Adrienne J. Sutton[1,2], Jan A. Newton[3], and Robert H. Byrne[4]

[1]Pacific Marine Environmental Laboratory, National Oceanic and Atmospheric Administration, Seattle, Washington, 98115, United States of America
[2]Joint Institute for the Study of the Atmosphere and Ocean, University of Washington, Seattle, WA, 98195, United States of America
[3]Applied Physics Laboratory, University of Washington, Seattle, Washington, 98105, United States of America
[4]College of Marine Science, University of South Florida, St. Petersburg, Florida 33701, United States of America
[*]Andrea.Fassbender@noaa.gov

Abstract

Evidence of ocean acidification (OA) throughout the global ocean has galvanized some coastal communities to evaluate carbonate chemistry variations closer to home. An impediment to doing this effectively is that, often, only one carbonate system parameter is measured at a time, while two are required to fully constrain the inorganic carbon chemistry of seawater. In order to leverage the abundant single-carbonate-parameter datasets in Washington State for more rigorous OA research, we have characterized an empirical relationship between total alkalinity (TA) and salinity ($TA = 47.7 \times S + 647$; $1\sigma = \pm 17$ μmol kg^{-1}) for regional surface waters (≤ 25 m) that is robust in the salinity range from 20-35 for all seasons. The relationship was evaluated using five years of 3-hour, contemporaneous observations of salinity, carbon dioxide partial pressure (pCO_2), and pH from a surface mooring on the outer coast of Washington. *In situ* pCO_2 observations and salinity-based estimates of TA were used to calculate pH for comparison with *in situ* pH measurements. On average, the calculated pH values were 0.02 units lower than the measured pH values across multiple pH sensor deployments, and showed extremely high fidelity in tracking the measured high-frequency pH variations. Our results indicate that the TA-salinity relationship will be a useful

tool for expanding single-carbonate-parameter datasets in Washington State and quality controlling dual pCO_2-pH time series.

Key Words

Total alkalinity; carbonate chemistry, Washington State; seawater pH

1. Introduction

Ocean acidification (OA) is the long-term decline in surface ocean pH resulting from the dissolution of anthropogenic carbon dioxide (CO_2) into seawater with subsequent hydration and deprotonation (Caldeira and Wickett 2003; Feely et al. 2004; Orr et al. 2005; Doney et al. 2009). OA has been observed widely throughout the open ocean (e.g., Rhein et al. 2013; Bates et al. 2014; Sutton et al. 2014; Lauvset et al. 2015); however, detecting pH declines in the coastal zone remains a challenge due to the high-magnitude, high-frequency, and irregular pH variations caused by natural and anthropogenic processes (Borges 2011; Hofmann et al. 2011; Takeshita et al. 2015). Recently OA in the natural environment has been linked to negative biological and economic impacts along the northwest coast of the United States (Adelsman and Binder 2012; Barton et al. 2012; Waldbusser et al. 2014; Barton et al. 2015). In this and other near-shore regions where local management strategies could be employed to address OA impacts (Kelly et al. 2011; Alin et al. 2015), more information is needed to identify where, why, and how fast seawater chemistry is changing so that effective adaptation and mitigation can be achieved (Boehm et al. 2015). Developing this type of modern baseline information often requires continuous and/or targeted sampling; however, in most coastal regions where carbonate system observations do exist, the data have been collected monthly or seasonally and provide only low temporal resolution information

in dynamically fluctuating environments. In addition, the carbonate system is complex and can vary in unpredictable ways in the coastal zone (Waldbusser and Salisbury 2014; Fassbender, Sabine, and Feifel 2016), which means that two parameters must be measured simultaneously to fully characterize the inorganic carbon chemistry of seawater (Millero 2007). Nevertheless, it is often the case that only one carbonate system parameter is measured at a time.

The carbonate system is commonly described by four principal components: dissolved inorganic carbon (DIC), total alkalinity (TA), pH, and carbon dioxide partial pressure (pCO_2). DIC is the sum of aqueous CO_2, carbonic acid, bicarbonate ion, and carbonate ion, which are the molecular species that result from the dissolution of CO_2 gas. TA is the excess of proton acceptors over proton donors in seawater with dissociation constants at 25 $^{\circ}$C and zero ionic strength that are below and above $10^{-4.5}$ respectively (Dickson 1981). Solution pH is the negative $\log_{10}$ of the hydrogen ion concentration, and pCO_2 is the partial pressure of CO_2 gas in equilibrium with seawater (Millero 2007). Measurement of any two of these parameters in addition to temperature, pressure, and salinity (as well as minor bases such as phosphate and silicate) makes it possible to fully constrain and calculate all other carbonate system components (Millero 2007; Dickson 2010a; Byrne 2014). This is necessary because different seawater carbonate chemistry conditions can result in identical values of pCO_2 or pH.

Techniques for laboratory determination of carbonate system parameters are somewhat mature (Dickson et al. 2007; Dickson 2010a; Dickson 2010b; Liu et al. 2011); however, autonomous observing capabilities are still developing. Within the past decade, autonomous pH and pCO_2 sensors have become commercially available (Martz et al. 2015). Although the strong negative

79 correlation between pH and pCO_2 renders this a challenging pair for constraining the carbonate
80 system (Dickson and Riley 1978; Millero 2007; Gray et al. 2011; Fassbender et al. 2015), due to
81 their availability, pH and pCO_2 sensors are providing the bulk of autonomous carbonate system
82 observations for the ocean carbon and acidification communities. In addition to fully autonomous
83 instrumentation, shipboard sensors for underway, continuous sampling have been increasingly
84 utilized over the past few decades (Feely et al. 1998; Pierrot et al. 2009; Sabine and Ducklow 2010;
85 Sabine et al. 2013) and measurements of surface ocean pCO_2 have grown exponentially (Pfeil et
86 al. 2013; Bakker et al. 2014). Isolated autonomous and shipboard measurements of pH or pCO_2
87 are often capable of providing important information about spatial and temporal trends and
88 variability (e.g., Hofmann et al., 2011; Sutton et al., 2014a, 2014b), but lack the information needed
89 for comprehensive characterization of the carbonate system.
90
91 A common way to leverage single-carbonate-system-parameter datasets, or make use of less-
92 than-ideal pH-pCO_2 measurement pairings, has been development of empirical relationships
93 between TA and salinity (e.g., Lee et al., 2006; Gray et al., 2011; Juranek et al., 2011; Fassbender,
94 2014; Takahashi et al., 2014; Fassbender et al., 2016; Xue et al., 2016). This approach is useful
95 due to dominance of TA variations driven by hydrologic cycles. In many open-ocean settings, TA
96 is a quasi-conservative property that scales linearly with salinity. In addition to the hydrologic
97 balance, TA in the surface ocean can be influenced by organic carbon transformations and, more
98 significantly, by calcium carbonate production and dissolution (Millero 2007; Fry et al. 2015).
99 With these considerations in mind, TA can be estimated from empirical relationships in near-shore
100 environments and used with *in situ* pH and/or pCO_2 observations to constrain and study the

carbonate system, provided that care is taken to account for the additional, and sometimes complex, influence of rivers.

Off the coast of Washington State and within the Salish Sea, research-cruise and platform-based time series (http://www.nanoos.org/) have been implemented to monitor the health of these marine waters (Feely et al. 2008; Feely et al. 2010; Alin et al. 2015). As a result, this region has a relatively large database of high-quality, ship-based, dual-carbonate-system-parameter data as well as an even larger database of single-carbonate-system-parameter data from moorings and underway measurement systems. Here we compile available high-quality hydrographic carbon data to develop a TA-S relationship within Washington's coastal marine surface waters and compare it to previous relationships developed for surface waters along the west coast of the United States (Lee et al. 2006; Gray et al. 2011; Wootton and Pfister 2012). Relying on *in situ* pH and pCO_2 observations from a mooring on the outer coast of Washington, we evaluate the performance of the TA-S relationship over a five year period. Finally, for pairing with pCO_2 or pH observations of varying accuracy, we evaluate how well TA must be determined to meet recently proposed data-quality objectives for ocean acidification monitoring in the coastal zone (Newton et al. 2014; McLaughlin et al. 2015).

2. Data Sources

2.1. Calibration Data: Cruise Observations

Discrete seawater samples for TA and salinity measurements collected at depths ≤ 25 m during Pacific Coast Ocean Observing System (PacOOS) cruises, National Oceanic and Atmospheric Administration (NOAA) Ocean Acidification Program (OAP) West Coast Ocean Acidification

(WCOA) cruises, and University of Washington (UW) cruises associated with the Puget Sound Regional Synthesis Model (PRISM) program, Washington Ocean Acidification Center (WOAC), and Northwest Association of Networked Ocean Observing Systems (NANOOS) and its Chá bă mooring were compiled for use as a calibration dataset in this analysis (**Figure 1, Table 1**). Full data and metadata for the four WCOA cruises are publically available on the Carbon Dioxide Information Analysis Center website (CDIAC: http://cdiac.ornl.gov; Feely and Sabine, 2011; Feely et al., 2014a, 2014b, 2015). PacOOS, PRISM, WOAC, and recent NANOOS data are currently being prepared for submission and will soon be publically available on the CDIAC and NANOOS (http://nvs.nanoos.org) websites.

The accuracy of discrete DIC and TA measurements (relative to Certified Reference Materials) during the WCOA cruises is reported as ±0.1% of the measurement value and the precision is reported as <±0.1% for TA and ~±1 µmol kg^{-1} for DIC. On average, the 0.1% accuracy level is equivalent to 2 µmol kg^{-1} ($1\sigma = \pm 0.1$ µmol kg^{-1}) for both DIC and TA throughout WA surface (<25 m) waters. PacOOS, PRISM, WOAC, and NANOOS carbon data used herein were analyzed at NOAA's Pacific Marine Environmental Laboratory and have similar accuracies and precisions. For simplicity we use ±2 µmol kg^{-1} as the total measurement uncertainty for all DIC and TA measurements. Discrete total-scale pH measurements were also made during the 2011 and 2013 WCOA cruises with measurement accuracies of ~±0.01 and precisions of ±0.0004. Cruise data with quality control flags of 2 or 6 (2=good data, 6=replicate samples) were used for the analysis.

Carbonate system calculations based on these data were made using the program CO_2SYS (Lewis and Wallace 1998; van Heuven et al. 2011) applying the constants of Lueker et al., (2000)

147 and Dickson, (1990) and the boron-to-chlorinity ratio of Uppstrom (1974). Approximately 20% of
148 the PRISM data do not include nutrient observations, so silicate and phosphate concentrations were
149 set to zero in CO_2SYS calculations for these samples. To estimate how missing nutrient
150 observations influence the accuracy of computed parameters, we calculated pH, pCO_2, and the
151 saturation state of aragonite (Ω_{Ar}) from DIC and TA using *in situ* nutrient concentrations and again
152 setting the nutrient concentrations to zero. pH and Ω_{Ar} values were lower by 0.009 and 0.02,
153 respectively, and pCO_2 values were higher by 17 µatm when nutrients were included in the PRISM
154 cruise calculations. Repeating the analysis using data from cruises other than PRISM yielded pH
155 and Ω_{Ar} values that were lower by 0.004 and 0.012, respectively, and pCO_2 values that were higher
156 by 6 µatm when nutrients were included. The PRISM calculations are approximately twice as
157 sensitive to nutrient input as the other cruises because most PRISM samples are collected within
158 Puget Sound and have nutrient concentrations nearly double those observed during other cruises,
159 on average. We will return to the discussion of these errors in Sections 3.4.2 and 3.5.
160
161 Of the 1,203 discrete TA bottle samples collected within the top 25 m of seawater at the stations
162 shown in **Figure 1**, only 10 have salinity values below 20. In addition, there are only a few
163 observations linking these low salinity values to the bulk of the samples, which lie above salinity
164 27 (~97%). As a result, we excluded these samples and have limited our analysis to the salinity
165 range of 20–35 to avoid curve fitting in undersampled regions of the TA-S domain. Average
166 monthly TA concentrations determined from the remaining 1,193 samples, as well as the sample
167 distribution by month, are shown in **Figure 2**. Based on these data, TA values appear to be highest
168 in summer and lowest in winter, with a notable exception in July due to a low salinity event within
169 the Strait of Juan de Fuca in 2008. Most of the TA samples were collected during the late summer

and early fall, with no observations from December or March and very few from January and June. Only during the months of May, August, September, and October have samples been collected in multiple years.

2.2. Validation Data: Mooring Observations

To validate the empirical relationship determined from cruise data, we used approximately five years of 3-hour surface water (~1 m) observations from the joint NANOOS-OAP Chá bă mooring located at 47.97°N, 124.95°W, offshore of La Push, Washington (**Figure 1**; Sutton et al., 2011). These include measurements of seawater temperature and salinity from a Sea-Bird Electronics (SBE) 16 conductivity-temperature-depth sensor, total-scale pH from a Sunburst Sensors SAMI^2 pH sensor, and sea surface and atmospheric boundary layer pCO_2 from a Battelle Memorial Institute Seaology® pCO_2 monitoring system (analogous to NOAA's MAPCO_2 system). All mooring data and metadata, excluding for pH, are accessible from the CDIAC and National Centers for Environmental Information (NCEI) websites. The pH observations from the Chá bă mooring are currently being prepared for submission to data archive centers for public access. The overall uncertainty of mooring pCO_2 measurements from the Seaology® system is ±2 µatm (Sutton, Sabine, et al. 2014). The accuracy of SBE 16 temperature and salinity values is <0.01 °C and <0.05, respectively. Quality control of Chá bă mooring pH measurements used herein will be addressed in Section 3.4.1. Carbonate system calculations based on these data were also made using the program CO_2SYS (Lewis and Wallace 1998; van Heuven et al. 2011) applying the previously mentioned constants. The concentrations of silicate and phosphate were set to zero for all of the CO_2SYS calculations performed using the validation dataset, which will be discussed further in Section 3.5.

3. Results and Discussion

3.1. Assessment of Organic Alkalinity

The commonly used definition for TA (Dickson 1981; Wolf-Gladrow et al. 2007) is largely governed by carbonate alkalinity with smaller contributions from borate and nutrients:

$$TA = [HCO_3^-] + 2[CO_3^{2-}] + [OH^-] - [H^+] + [B(OH)_4^-] + [HPO_4^{2-}] + 2[PO_4^{3-}] - [H_3PO_4] + [SiO(OH)_3^-] + \ldots \quad (\mathbf{1})$$

In the coastal zone, organic acids originating from terrestrial runoff and/or phytoplankton blooms can contribute additional alkalinity (Org-Alk; Cai et al., 1998), complicating the interpretation of TA measurements (Kim et al. 2006; Hernandez-Ayon et al. 2007; Muller and Bleie 2008; Hunt et al. 2011; Yang et al. 2015). Software packages for seawater carbonate system chemical equilibria, such as CO_2SYS (Lewis and Wallace 1998; van Heuven et al. 2011) account for carbonate, hydroxide, borate, and nutrient contributions to TA, assuming Org-Alk is negligible. Therefore, quantifying the Org-Alk contribution to TA in coastal regions is needed to determine whether parameters calculated from measured TA may be artificially affected by alkalinity contributions that have not be accounted for in CO_2SYS (e.g., Kuliński et al. 2014; Yang et al. 2015). Compounding the issue, inorganic alkalinity and Org-Alk can be unique to specific rivers or regions (Hunt et al. 2011; Abril et al. 2015; Yang et al. 2015), vary both seasonally and interannually (e.g., Figure 2 in Evans et al., 2013), and be influenced by land use or climatic changes on decadal timescales (Raymond and Cole 2003; Raymond et al. 2008; Hu et al. 2015). This means that a single TA-salinity (TA-S) relationship may not be appropriate indefinitely or for

a broader coastal region, as discussed by Friis et al. (2003) at the ocean-basin scale. While this poses challenges for the empirical TA-S approach in near-shore environments, the potential utility of coastal TA estimates for investigators working with limited, single-carbonate-system-parameter datasets to address OA is significant.

Prior to evaluating regional TA-S relationships, the influence of Org-Alk on TA measurements must be considered. During the 2011 and 2013 WCOA cruises, the carbonate system was over-constrained through the redundant measurement of TA in addition to DIC and total-scale pH (Feely and Sabine 2011; Feely et al. 2015). Following Hunt et al. (2011) and Yang et al., (2015), we assessed the Org-Alk contribution to TA by subtracting the alkalinity calculated from DIC and pH from direct measurements of TA:

$$\text{Org-Alk} = TA_M - TA_C \quad (\mathbf{2})$$

Direct measurement of TA (TA_M) includes all alkalinity contributions, while calculations of TA (TA_C) only account for carbonate, hydroxide, borate, and nutrient alkalinity. Therefore, the difference between the two represents the Org-Alk contribution. This approach for estimating Org-Alk is only feasible due to the compatibility of pH measurements and Lueker et al., (2000) carbonate system equilibrium constants, which both use total-scale pH.

After removing the largest single outlier from each cruise estimate, the average Org-Alk and 1σ values for the outer coast samples are 5 ± 5 μmol kg^{-1} (2011, n = 64) and 3 ± 6 μmol kg^{-1} (2013, n = 72), and Org-Alk was not strongly correlated with salinity (R^2<0.09). Propagating DIC and pH

measurement uncertainties (see Section 2.1) through the CO_2SYS calculations of TA using a Monte Carlo approach yields a 1σ TA_C uncertainty of ±4.4 μmol kg^{-1}. Coupling this with a ±2 μmol kg^{-1} measurement uncertainty for TA_M gives an Org-Alk computational uncertainty of ~±5 μmol kg^{-1}. This indicates that, on average, Org-Alk concentrations are not statistically distinguishable from zero.

At present, our analysis of Org-Alk is notably constrained to two cruises along the outer coast of Washington, since it is very rare that three carbonate system parameters are measured simultaneously. In addition, all of the samples used to determine Org-Alk were collected during the month of August after peak Columbia River discharge, which occurs in June. The Columbia River is the second largest river in the continental United States and dominates freshwater input along the outer coast of Washington (Hickey et al. 2005; Hickey and Banas 2008). TA in the Columbia River varies seasonally with an average summer concentration of ~1000 μmol kg^{-1} (Evans et al. 2013). The average salinity of samples used in the Org-Alk analysis is ~32 ± 1, indicating that river input was almost negligible during each of the WCOA cruises - limiting our ability to assess the importance of river-derived Org-Alk in the region. Therefore, further work is needed to quantify the temporal and spatial variability of Org-Alk throughout Washington, including the Salish Sea where numerous rivers drain.

3.2. Regression Analysis

Linear-least-squares regressions were performed on the calibration data using the Matlab *robustfit* function. The measured TA (TA_M - simply referred to as TA from here on) was initially regressed against temperature and salinity using a multiple linear regression (MLR) analysis;

however, direct regression with salinity yielded the lowest residuals and highest correlation coefficient. Following the MLR approach, Analysis of Covariance (Matlab *aoctool* function) was used to identify more targeted spatial and temporal relationships between TA and salinity. TA-S relationships were evaluated by season and for the following geographical regions: Outer Coast, Hood Canal, South Sound, Whidbey Basin, Central Sound, and Strait of Juan de Fuca (**Figure 1**). Two distinct seasonal regressions were observed; one for the May to October period, overlapping with seasonal upwelling (e.g., Feely et al., 2008, 2010), and one for the November to April period. At the time of this analysis, however, no data were available for the months of March and December, and there are significantly more observations between May and October than between November and April (**Table 2**). The regional evaluation also resulted in two distinct relationships in which the South Sound was grouped with the Outer Coast rather than a neighboring region, likely due to data sparsity. While acknowledging that additional data may lead to tighter seasonal or regional regressions in the future, due to the skewed spread in observations, seasonally and by basin (**Figure 2; Table 2**), we have conservatively elected to use a single regression for the entire region.

To ensure internal consistency of the WA TA-S relationship we used a Cross-Validation approach in which a Monte Carlo loop was constructed to randomly select 90% of the calibration data for regression development and 10% for validation over 1,000 computational repetitions. This yielded a mean, statistically significant regression ($r^2 = 0.95$, $p<0.001$):

$$TA = 47.7(\pm 0.2) \times S + 647(\pm 6) \quad (\mathbf{3})$$

with a mean residual and 1σ variation of 1 ± 17 μmol kg^{-1} (**Figure 3**; coefficient standard errors given in (**3**)). The 2σ uncertainty (95% confidence limit) in the TA-S regression is ±34 μmol kg^{-1}, which reflects TA variations caused by processes other than dilution and evaporation, such as photosynthesis and respiration, calcium carbonate precipitation and dissolution, mixing, and Org-Alk contributions to TA. The slope of the WA regression line deviates significantly from the slope of the dilution line ($\partial TA\ \partial S^{-1}$ ~68 μmol kg^{-1}), which is the TA-S relationship that would result if seawater were diluted with freshwater containing 0 μmol kg^{-1} TA. This observation, along with the regression y-intercept of 647 μmol kg^{-1}, indicates that regional rivers add substantial alkalinity to near-shore ocean waters. To test the depth dependence of the TA-S relationship, we repeated the regression analysis using data from the top 5 m of water and found a statistically indistinguishable relationship that had a larger mean residual and 1σ variation (2 ± 43 μmol kg^{-1}) due to the smaller sample size (n = 396). This indicates that the 25 m TA-S relationship is representative of near-surface conditions within the stated level of uncertainty.

3.3. Comparison of Regional TA-S Relationships

Comparison of the WA TA regression with other TA-S relationships from the broader region reveals notable differences in the slopes and intercepts (**Table 3**, **Figure 4**). Using the same discrete TA and salinity samples from which the WA TA-S relationship was constructed, we calculate TA from the other empirical relationships and compare their accuracies (**Table 3**). The regressions from Lee et al. (2006) and Gray et al. (2011) (referred to as KL and CG hereafter) yield TA estimates that are biased slightly low; however, the estimates are not statistically different from the observations. The Wootton and Pfister, (2012) regression (referred to as TW hereafter) gives TA estimates that are biased high and that are significantly different from the observations. This

is noteworthy because the KL and CG algorithms are for the broader North Pacific Ocean and the central California coast near Monterey, respectively, while the TW regression was developed using data from Washington waters off the Strait of Juan de Fuca. The TW regression was based on the fewest samples (n = 36), and may therefore be data-limited or seasonally biased; however, it is also possible that a different, local TA-S relationship exists near the northernmost tip of the Washington outer coast.

Results from the comparison analysis suggest that, in the salinity range of 20–35, the WA specific TA-salinity relationship is not statistically different from the CG and KL relationships; although, the 1σ magnitude of the TA residuals is ~75% larger for the KL relationship than for the WA and CG relationships. Importantly, most of the samples used for this comparison have salinities above 27 (**Figure 3**), which does not capture the large positive bias of the KL algorithm and smaller negative bias of the CG algorithm below salinity ~27 (**Figure 4**). In light of these biases in the lower range of the salinity domain, in the absence of a location-specific TA-S relationship the WA TA-salinity relationship should be used for samples collected within the 20–35 salinity range from Washington waters.

3.4. Testing the WA TA-S Relationship at the Chá bă Mooring

The NANOOS-OAP Chá bă mooring provides a unique opportunity to validate the WA TA-S relationship identified herein. This dual-carbonate-system-parameter (pH and pCO_2) time series makes it possible to estimate TA using the WA TA-S relationship and, with the *in situ* pCO_2 measurements, calculate pH as well as Ω_{Ar}. The calculated pH values can be directly compared with *in situ* measurements of pH from the mooring to determine how well the WA TA-S relationship holds at a specific site for an extended period of time. In addition, discrete DIC and

TA bottle samples collected near the Chá bă mooring throughout the time series are used to calculate pH and Ω_{Ar} for comparison with the calculated and measured mooring values.

3.4.1. Quality Control of *in situ* pH Data

While quality control (QC) procedures have been standardized for autonomous pCO_2 measurements made by the Seaology® system (Sutton et al. 2014) used on the Chá bă mooring, QC procedures for the Sunburst SAMI^2 pH sensor have not yet been developed for community-wide, end-user application beyond the basic sensor component failure recognition provided by the manufacturer. To develop this QC procedure, pH observations were converted to hydrogen ion concentrations [H^+] and plotted against pCO_2, revealing their strong correlation (**Figure 5A**; Dickson and Riley, 1978). Because these parameters are influenced by all of the same processes (e.g., respiration, CO_2 gas exchange, photosynthesis, calcification, dilution, etc.), any change in pCO_2 should be accompanied by a coordinated change in [H^+], making this a strategic way to identify outliers. By viewing the data in this way, a negative bias in the 2012–2013 SAMI^2 pH measurements (positive bias in [H^+] space) was revealed (**Figure 5A**). To correct the bias, we fit a linear, least-squares regression to data collected during the other deployment years and determined the mean offset between the fit and the 2012–2013 deployment [H^+] values. The biased data were then adjusted by the [H^+] offset to fall in line with the observed [H^+]-pCO_2 relationship (**Figure 5B**). After accounting for sensor biases, the strong covariance between [H^+] and pCO_2 was used to further identify outliers in the dataset. A linear, least-squares regression was fit to the corrected dataset and a conservative ±3σ window around the fit (1σ = ±0.22 nmol kg^{-1}) was used to flag data outside of the window as outliers, which were removed from the analysis (**Figure 5C**). **Figure 5D** shows both the corrected and final pH datasets vs. pCO_2.

By using $[H^+]$ instead of pH during the determination of outliers the y-axis is symmetric, which would not be the case in logarithmic space. For example, consider using a pH window of ±0.06 around the observed pH-pCO_2 relationship. At any pH level, the $[H^+]$ change associated with +0.06 pH will be a smaller in magnitude than the $[H^+]$ change associated with -0.06 pH. In addition, the $[H^+]$ change associated with -0.06 (and +0.06) pH will be a larger magnitude at low-pH values relative to high-pH values, which would result in a relaxation of the outlier window in the lower-pH range. Therefore, to avoid biasing datasets towards the inclusion of more outliers in the lower-pH range than higher-pH range, it is advised to perform this type of quality control in $[H^+]$ space.

While this may appear to be a convenient way to QC *in situ* pH data that are collected alongside *in situ* pCO_2 observations, our analysis benefits from two very important characteristics. At this location, we have five years of *in situ* observations with which to constrain the $[H^+]$-pCO_2 relationship. This data density allows us to capture variability in the slope of $[H^+]$-pCO_2 relationship caused by various processes that may occur at different times of year (e.g., Figure 3 in Gray et al., 2011). These processes broaden the extent of the $[H^+]$-pCO_2 relationship, such that we don't accidently exclude viable data when trying to identify outliers. In the absence of a long time series, this type of QC analysis may still be applied by dividing data into deployment segments and relying on well calibrated or validated portions of the dataset as well as auxiliary information (e.g., oxygen, nutrients, chlorophyll, and turbidity) to discern various processes that may be influencing the $[H^+]$-pCO_2 relationship. In addition to a long time series, one of the primary reasons this analysis is feasible is due to the high quality of pCO_2 data achievable from the Seaology® system, even during extended duration deployments. Perhaps the most unique and,

arguably, critical feature of the Seaology® system is its ability to resist biofouling: a copper-nickel pipe is the only component that touches the seawater (Sutton et al. 2014). If pH and pCO_2 sensors at a given site are influenced by biofouling, and more importantly and likely, if the influence is dissimilar between sensors, the pH-pCO_2 relationship may be heavily biased or even indiscernible. Therefore, the method presented here should be applied with caution and only to appropriate datasets with well-validated pCO_2 observations or where high-quality discrete samples can be used to supplement *in situ* observations. Although we have focused this discussion using pCO_2 as the confirmed parameter, this approach could work equally well using pH measurements of known quality, converted to $[H^+]$, as the confirmed parameter to assess the accuracy of contemporaneous pCO_2 measurements.

3.4.2. Comparing Calculated and Measured pH at the Chá bă Mooring

The WA TA-S relationship was applied to salinity observations (**Figure 6A**) from the Chá bă mooring to calculate a time series of TA (TA_S; **Figure 6B**) that was used with *in situ* pCO_2 observations (**Figure 6C**) to calculate Ω_{Ar} and pH (pH_C). In addition, 13 discrete TA and DIC bottle samples collected from the top 5 m of water within ±0.05° longitude and ±0.07° latitude of the buoy and 12 hours of an *in situ* mooring observation were used for comparison. On average, salinity values from the discrete bottle samples are ~0.40 units higher than the mooring salinity observations, and bottle TA values are ~15 µmol kg^{-1} higher than the TA_S estimates. Most of the discrete samples were collected ~1 nautical mile from the buoy location and within 2 hours of a mooring observation, so differences between sensor measurements and bottle samples may reflect spatial and/or temporal variability in surface waters. In addition, the mooring sensor measurements occur at ~1 m, while bottle sample depths ranged from ~1 to 5 m with a mean depth of ~3 m, which

means that vertical stratification may also contribute to the observed offset. Assuming that differences in salinity between the mooring and bottle samples were caused by conservative processes (evaporation and precipitation or conservative mixing), we can calculate the expected TA offset. Using the average TA/S ratio for the discrete samples (68.6) and multiplying by the mean 0.40 salinity difference gives an expected TA difference of 27 µmol kg^{-1}. Thus, the ~15 µmol kg^{-1} offset between discrete TA samples and TA_S estimates is close to what could be expected, and is within the 1σ TA-S regression uncertainty (1σ = ±17).

Ω_{Ar} values calculated from TA_S and *in situ* pCO_2 remain above 1 for the entire observational period, with values ranging from ~1 to 4.5 (**Figure 6D**). The range and seasonality of Ω_{Ar} values agree with a recent, independent assessment of the Ω_{Ar} monthly climatology determined using *in situ* pCO_2 and pH measurements from the Chá bă mooring (Sutton et al. 2016). Calculations of Ω_{Ar} from the discrete bottle samples are 0.13 units lower than the mooring estimates on average. With higher TA and lower Ω_{Ar} values for the discrete bottle samples relative to the mooring values, bottle derived pH values are expected to be lower than the mooring values, as is observed. Discrete pH values calculated from the DIC and TA bottle samples are 0.06 pH units lower than the measured values after quality control ($pH_{M\ QC}$) and 0.03 pH units lower than the calculated (pH_C) values (**Figure 7A**). The discrete pH values have a calculation uncertainty of ±0.007 and pH_C values calculated from TA_S (1σ = ±17 µmol kg^{-1}) and pCO_2 (uncertainty = ±2 µatm) have a calculation uncertainty of ~±0.005. The manufacturer stated accuracy of the $SAMI^2$ pH sensor is ±0.003 and the absence of nutrient data in CO_2SYS calculations from the DIC-TA pair can lead to pH biases of up to ~-0.009 (Section 2.1). All of these errors combined cannot account for the 0.06 and 0.03 pH differences between moored and discrete observations. This is not surprising since

the nearby bottle samples did not perfectly reflect seawater conditions at the exact time, location, and depth of the mooring sensor (as evidenced by the 0.4 salinity difference). Therefore, it is likely that the sensor values more accurately represent conditions at the mooring, particularly in the patchy and rapidly changing chemical environment of the coastal ocean.

Figure 7B shows the difference between calculated and measured pH values at the Chá bă mooring, before and after quality control of the pH measurements. The $pH_{M\ QC}$ values are consistently ~0.02 pH units higher than pH_C values across seasons and deployments. This pH difference also cannot be accounted for by the pH errors mentioned in the previous paragraph. Consistency in this bias across all SAMI^2 pH sensor deployments would suggest that it is not caused by the sensors and instead either reflects an error in TA_S or pCO_2 that is greater than what we have accounted for (e.g., ±17 µmol kg^{-1} and ±2 µatm, respectively), or is caused by a discrepancy in sample depths. In order to attain a pH offset of 0.02, there would need to be a pCO_2 measurement bias on the order of 10–15 µatm, a TA_S bias on the order of -100 µmol kg^{-1}, or a combination of biases in both parameters. Alternatively, the WA TA-S relationship is based on samples collected within the top 25 m of the water column while the moored sensor samples at ~1 m. Although we did not find a significant depth bias in the overall WA TA-S relationship (Section 3.2), differences in sample depth may contribute to a bias in TA_S and, thus, in pH_C near the Chá bă mooring.

Perhaps most importantly, the calculated and measured pH values show nearly identical temporal variability throughout the time series. A zoom in of the summer 2012 Chá bă mooring deployment shows this clearly (**Figure 7C)**. This means that high-frequency (3-hour intervals in

this case) carbonate chemistry information can be reproduced precisely when using the TA-S relationship with high-quality and –frequency pCO_2 observations. Additionally, the high fidelity of calculated pH suggests that another application of the TA-S relationship is the quality control of *in situ* pH observations at other time-series locations in Washington: particularly since the TA-S relationship is not affected by biofouling.

For this application, sensor pH data were QC'd using contemporaneous pCO_2 observations and then compared with calculated pH values in Section 3.4.2. This was done to avoid circularity since we were evaluating how well calculated pH values compared with *in situ* observations. For future data QC purposes, however, pH should first be calculated from TA_S and pCO_2 and directly compared with the measured pH values to identify biases that may be more challenging to see in $[H^+]$ vs. pCO_2 space (e.g., **Figure 7B** gray symbols vs. **Figure 5A**). Once the biased data are adjusted, then the $[H^+]$ values should be plotted against pCO_2 for more rigorous QC (e.g., **Figure 5C**).

3.5. Accuracy Requirements to Meet Specified OA Monitoring Needs

Recently, the California Current Acidification Network (C-CAN) held a series of workshops on OA that resulted in the recommendation to use aragonite saturation state (Ω_{Ar}) as a common carbonate system currency to compare data from OA monitoring efforts throughout the California Current System (CCS; McLaughlin et al., 2015). Aragonite is a metastable form of the mineral calcium carbonate ($CaCO_3$) used by many marine organisms to make their shells (e.g., Fabry et al., 2008, 2009). Aragonite saturation state (Ω_{Ar}) is a commonly used parameter to describe the thermodynamic potential of this mineral to dissolve, and is defined as:

$$\Omega_{Ar} = \frac{[Ca^{2+}]\,[CO_3^{2-}]}{K_{sp}'} \quad (4)$$

where the temperature, pressure, and salinity dependence of the apparent solubility product (K_{sp}') is taken from Mucci (1983), and [Ca^{2+}] and [CO_3^{2-}] are seawater concentrations of calcium and carbonate ions. Ω_{Ar} values < 1 indicate that aragonite is thermodynamically unstable and will begin to dissolve, while values ≥ 1 indicate that aragonite is thermodynamically stable in the environment.

While Ω_{Ar} cannot be measured directly at present, McLaughlin et al., (2015) suggest that computational accuracies of ±0.2 for Ω_{Ar} and measurement accuracies of ±0.02 for pH may be "technologically achievable and biologically meaningful goals" for OA monitoring in the CCS. These goals are equivalent to the Global Ocean Acidification Observing Network (GOA-ON) data-quality objectives for carbonate system "weather," which refers to relative spatial patterns in carbonate chemistry as well as short-term responses to local OA dynamics (Newton et al. 2014). In addition to "weather," GOA-ON also defined "climate" data-quality objectives, where "climate" refers to long-term trends in carbonate-system parameters, and particularly OA. The "climate" objectives include measuring pH with an accuracy of 0.003 and calculating Ω_{Ar} with a relative uncertainty of 1%. In consideration of these recommendations, we explored the utility of the WA TA-S relationship for computing Ω_{Ar}, pCO_2, and pH when paired with pH and pCO_2 observations of differing accuracies.

Observations from the NANOOS-OAP Chá bă mooring (**Figure 1**) collected between June 2010 and June 2014 are used for this analysis. Approximately 6,900 samples were recorded over this time period with salinities ranging from 22.7 to 32.6, temperatures from 7.0 to 18.8 °C, and pCO_2 from 100 to 640 µatm. Ω_{Ar}, pCO_2, and pH were calculated from TA_S and *in situ* pH and pCO_2 measurements taking a Monte Carlo approach in which six ascending, hypothetical errors for TA, pH, and pCO_2 were propagated through the calculations. Input errors ranged from 0 to 100 µmol kg^{-1} for TA, from 0 to 0.02 for pH, and from 1 to 10 µatm for pCO_2. The errors for each parameter were varied independently and at random (in a Gaussian distribution) within ~±3 times the error magnitude, before being added to the TA, pH, and pCO_2 values used to calculate Ω_{Ar}, pCO_2, and pH. This process was completed 250 times for each parameter pairing and the standard deviation of the 250 resultant estimates of Ω_{Ar}, pCO_2, and pH for each of the ~6,900 observations was determined. These ~6,900 standard deviations were then averaged for each parameter, giving an estimate of the accuracy achievable from the input TA and pH or pCO_2 values (and their associated errors) within the temperature and salinity range of the observations (**Figure 8**).

The results indicate that GOA-ON and C-CAN "weather" data-quality objectives can be achieved for pH and Ω_{Ar} in Washington waters. For pH, this requires using TA values with an uncertainty ≤ 100 µmol kg^{-1} paired with pCO_2 observations with an uncertainty ≤ 5 µatm (**Figure 8A**). For Ω_{Ar}, this requires using TA values with an uncertainty ≤ 100 µmol kg^{-1} paired with pCO_2 observations with an uncertainty ≤ 10 µatm (**Figure 8C)**. Similarly, the Ω_{Ar} "weather" data-quality objective can be achieved when calculated from pH and pCO_2 values that have measurement uncertainties of ≤ 0.015 and ≤ 5 µatm, respectively (**Figure 8D**). In order to achieve the GOA-ON "climate" data-quality objectives for pH and Ω_{Ar}, TA must be known to 10 µmol kg^{-1} or better and

paired with pCO_2 observations that have uncertainties ≤ ~2 µatm (**Figure 8C**). With a 2σ of ±34 µmol kg^{-1}, the WA TA-S relationship is not sensitive enough to achieve this data-quality objective, even when paired with high-quality pCO_2 measurements. Finally, **Figure 8B** shows the uncertainty in pCO_2 when calculated from TA and pH in Washington's coastal waters using a range of uncertainties for these parameters.

Calculations of pH and Ω_{Ar} are more sensitive to the input pCO_2 errors than TA errors and calculations of pCO_2 are more sensitive to the input pH errors than TA errors (**Figure 8**). This means that the accuracy of *in situ* pCO_2 and pH measurements will be critical for achieving high-quality estimates of pH, pCO_2, and Ω_{Ar} when using the TA-S relationship. Furthermore, in order to compete with Ω_{Ar} values calculated from TA_S and mid-quality pCO_2 measurements (uncertainty ~±10 µatm), pH must be measured to an accuracy ≤ 0.01 and paired with pCO_2 observations with an accuracy ≤ 5 µatm. The requirement of higher-accuracy pH and pCO_2 measurements for the Ω_{Ar} calculation exemplifies the challenge when using this pair to constrain the carbonate system. To summarize, even low accuracy TA estimates will be useful for leveraging pCO_2 (pH) observations to calculate pH (pCO_2) or Ω_{Ar} in Washington's coastal waters with salinities above 20, even when pCO_2 and pH have been measured simultaneously.

Nutrient concentrations were set to zero for all CO_2SYS calculations made using Chá bă mooring data, since 3-hour, *in situ* measurements of phosphate and silicate are not taken at the mooring. The sensitivity of CO_2SYS calculations to nutrient input was evaluated in Section 2.1, and findings suggest that the absence of nutrients data can result in pH, Ω_{Ar}, and pCO_2 biases of ~0.009, ~0.02, and -17 µatm in nutrient rich areas (e.g., Puget Sound). However, these sensitivity

estimates were made using DIC and TA as the calculation input parameters and our analysis of errors in Section 3.5 is conducted using TA-pCO_2 and TA-pH pairs of input parameters. To evaluate the sensitivity of CO_2SYS calculations to nutrient input for the TA-pH pair, we used discrete TA, pH, and nutrient observations from the 2011 and 2013 WCOA cruises. Results yielded Ω_{Ar} and pCO_2 values that were lower by 0.0005 and <1 µatm when nutrients were included. For reference, the DIC-TA input pair yielded differences in Ω_{Ar}, pH, and pCO_2 of -0.004, -0.011 and 7 µatm, respectively, when nutrients were included for the same cruises. Although we do not have independent pCO_2 observations from these cruises to test the TA-pCO_2 pair, due to the tight correlation between pH and pCO_2, we expect similar results. Therefore, the influence of absent nutrient data on carbonate system calculations made with TA-pCO_2 and TA-pH pairs of input parameters is negligible relative to measurement uncertainties at this location.

Our results indicate that the C-CAN and GOA-ON pH "weather" data-quality objective of ±0.02 for pH can be attained when calculated using the WA TA-S relationship and high-quality, *in situ* measurements of pCO_2. Being able to accurately replicate the frequency and magnitude of pH fluctuations in Washington waters using the TA-S relationship with the vast number of pCO_2 observations from moorings and volunteer observing ships will make it possible to characterize regional and temporal pH variability. This baseline information can then be used to design strategic monitoring efforts that will increase our understanding of the system and allow us to determine when and where the OA signal may be discernable. In addition, information of this type will be particularly valuable to scientists studying the effects of OA on organisms, since it will provide additional context for the range and duration of pH exposure organisms already endure.

4. Conclusions

Using high-quality, dual-carbonate-system-parameter datasets, we have identified an empirical relationship between total alkalinity (TA) and salinity for surface waters (≤ 25 m) near Washington State. The TA-salinity (TA-S) relationship appears robust for all seasons in the salinity range from 20–35. Estimates of TA derived from this relationship can be used to calculate pH and Ω_{Ar} and meet the GOA-ON and C-CAN proposed carbonate system "weather" data-quality objectives (Newton et al. 2014; McLaughlin et al. 2015) when paired with pCO_2 observations that have an uncertainty of up to 10 µatm (and higher). Due to the abundance of high-accuracy, single-carbonate-system-parameter data that exists in Washington, as well as other coastal states, this approach provides a pragmatic mechanism to produce a second parameter for full determinations of seawater carbonate chemistry.

Although the WA TA-S relationship will be an important tool for expanding the quantity of data available for regional OA research, a few important caveats and considerations should be reiterated here. The regression captures the mean TA-S relationship for the region in both time and space; however, at various times of year, processes that are independent of the hydrologic cycle can influence TA without influencing salinity. These processes include photosynthesis and respiration as well as calcium carbonate precipitation and dissolution. Careful consideration of how these biological processes may influence the interpretation of a small or seasonally-biased dataset relying on the TA-S relationship is needed. In addition to biological considerations, changes in riverine TA (organic or other forms of alkalinity) on seasonal, annual, or decadal time scales could lead to unexpected changes in the TA-S relationship both temporally and spatially (e.g., Raymond and Cole 2003; Raymond et al. 2008; Hu et al. 2015). Due to the complexity of

carbonate chemistry near river mouths (Waldbusser and Salisbury 2014) more investigations are needed in these regions. Specifically, observations spanning the full dynamic range of variability throughout the year will be required to determine the reliability of the TA-S approach in river-influenced contexts. Finally, the method used herein relies on having a significant number of high-quality, calibration samples (n=1,993) that span all seasons, which may not be easily obtained in all regions of investigation. Local environmental characteristics, data quality, validation capabilities, and accuracy goals should be taken into account when developing this type of method to leverage single-carbonate-system-parameter data in the coastal zone.

5. Acknowledgements

We thank the crew and science parties on all cruises that contributed to this work, which represent University of Washington (UW) Puget Sound Regional Synthesis Model (PRISM) program, Northwest Association of Regional Ocean Observing Systems (NANOOS), and Washington Ocean Acidification Center (WOAC) cruises focused on Washington waters, as well as NOAA's West Coast Ocean Acidification cruises and NOAA Fisheries-led PacOOS cruises focused on the outer coast. We are grateful to Beth Curry for her efforts in compiling and quality controlling the UW cruise data. The moored time-series observations benefited from the technical expertise of John Mickett, Sylvia Musielewicz, and Randy Bott. Funding for cruise and mooring observations used in this paper came from the NOAA Ocean Acidification Program, NOAA Global Carbon Cycle Program, NOAA Climate Observation Division in the Climate Program Office, NOAA Fisheries, U.S. Integrated Ocean Observing System (IOOS) through NANOOS, Washington State funded WOAC, and UW PRISM Program. The authors were supported by the Postdocs Applying Climate Expertise (PACE) Fellowship Program, partially funded by the NOAA Climate Program Office and administered by the UCAR Visiting Scientist Programs; NOAA Pacific Marine Environmental Laboratory; WOAC and NANOOS via U.S. IOOS. This manuscript benefitted from the input of three anonymous reviewers and is PMEL contribution number 4473.

6. References

Abril, G., S. Bouillon, F. Darchambeau, C. R. Teodoru, T. R. Marwick, F. Tamooh, F. Ochieng Omengo, et al. 2015. Technical Note: Large overestimation of pCO_2 calculated from pH and alkalinity in acidic, organic-rich freshwaters. *Biogeosciences* 12: 67–78. doi:10.5194/bg-12-67-2015.

Adelsman, H., and L. Whitely Binder. 2012. *Ocean Acidification: From Knowledge to Action,*

Washington State's Strategic Response. Olympia, Washington.

Alin, S.R., R. Brainard, N. Price, J.A. Newton, A. Cohen, W. Peterson, E. DeCarlo, E. Shadwick, S. Noakes, and N. Bednaršek. 2015. Characterizing the Natural System: Toward Sustained, Integrated Coastal Ocean Acidification Observing Networks to Facilitate Resource Management and Decision Support. *Oceanography* 25: 92–107. doi:10.5670/oceanog.2015.34.

Bakker, D. C. E., B. Pfeil, K. Smith, S. Hankin, A. Olsen, S.R. Alin, C. E. Cosca, et al. 2014. An update to the Surface Ocean CO_2 Atlas (SOCAT version 2). *Earth System Science Data* 6: 69–90. doi:10.5194/essd-6-69-2014.

Barton, A., B. Hales, G. G. Waldbusser, C. Langdon, and R.A. Feely. 2012. The Pacific oyster, Crassostrea gigas, shows negative correlation to naturally elevated carbon dioxide levels: Implications for near-term ocean acidification effects. *Limnology and Oceanography* 57: 698–710. doi:10.4319/lo.2012.57.3.0698.

Barton, A., G. G. Waldbusser, R.A. Feely, S. B. Weisberg, J.A. Newton, B. Hales, S. Cudd, et al. 2015. Impacts of Coastal Acidification on the Pacific Northwest Shellfish Industry and Adaptation Strategies Implemented in Response. *Oceanography* 25: 146–159. doi:10.5670/oceanog.2015.38.

Bates, N.R., Y.M. Astor, M.J. Church, K. Currie, J.E. Dore, M. González-Dávila, L. Lorenzoni, F. Muller-Karger, J. Olafsson, and J.M. Santana-Casiano. 2014. A time-series view of changing surface ocean chemistry due to ocean uptake of anthropogenic CO_2 and ocean acidification. *Oceanography* 27: 126–141. doi:http://dx.doi.org/10.5670/oceanog.2014.16.

Boehm, A.B., M.Z. Jacobson, M. O'Donnell, M. Sutula, W. W. Wakefield, S. B. Weisberg, and E. Whiteman. 2015. Ocean Acidification Science Needs for Natural Resource Managers of the North American West Coast. *Oceanography* 25: 170–181. doi:10.5670/oceanog.2015.40.

Borges, A V. 2011. Present Day Carbon Dioxide Fluxes in the Coastal Ocean and Possible Feedbacks Under Global Change. In *Oceans and the Atmospheric Carbon Content*, ed. Pedro Duarte and J. Magdalena Santana-Casiano, 47–77. Dordrecht: Springer Netherlands. doi:10.1007/978-90-481-9821-4_3.

Byrne, R.H. 2014. Measuring ocean acidification: New technology for a new era of ocean chemistry. *Environmental Science and Technology* 48: 5352–5360. doi:10.1021/es405819p.

Caldeira, K., and M.E. Wickett. 2003. Anthropogenic Carbon and Ocean pH. *Nature* 425: 365–365. doi:10.1038/425365a.

Dickson, A.G. 1981. An exact definition of total alkalinity and a procedure for the estimation of alkalinity and total inorganic carbon from titration data. *Deep Sea Research Part A. Oceanographic Research Papers* 28: 609–623. doi:10.1016/0198-0149(81)90121-7.

Dickson, A.G. 1990. Standard potential of the reaction : $AgCl(s) + 1/2H_2(g) = Ag(s) + HCl(aq)$, and the standard acidity constant of the ion HSO_4^- in synthetic sea water from 273.15 to 318.15 K. *Journal of Chemical Thermodynamics* 22: 113–127.

Dickson, A.G. 2010a. Seawater carbonate chemistry. In *Guide to best practices for ocean*

acidification research and data reporting, 17–40.

Dickson, A.G. 2010b. Standards for Ocean Measurements. *Oceanography* 23: 34–47. doi:10.5670/oceanog.2010.22.

Dickson, A.G., and JP Riley. 1978. The effect of analytical error on the evaluation of the components of the aquatic carbon-dioxide system. *Marine Chemistry* 6: 77–85. doi:10.1016/0304-4203(78)90008-7.

Dickson, A.G., C.L. Sabine, and J.R. Christian, ed. 2007. *Guide to best practices for ocean CO_2 measurements*. *PICES Special Publication 3, 191*. PICES Special Publication 3, 191 pp.

Doney, S. C., V. J. Fabry, R.A. Feely, and J.A. Kleypas. 2009. Ocean acidification: the other CO_2 problem. *Annual review of marine science* 1: 169–192. doi:10.1146/annurev.marine.010908.163834.

Evans, W., B. Hales, and P.G. Strutton. 2013. pCO_2 distributions and air-water CO_2. *Estuarine, Coastal and Shelf Science* 117: 260–272. doi:10.1016/j.ecss.2012.12.003.

Fabry, V. J., J. McClintock, J.T. Mathis, and J. Grebmeier. 2009. Ocean Acidification at High Latitudes: The Bellwether. *Oceanography* 22: 160–171. doi:10.5670/oceanog.2009.105.

Fabry, V. J., B. A. Seibel, R.A. Feely, and J. C. Orr. 2008. Impacts of ocean acidification on marine fauna and ecosystem processes. *ICES Journal of Marine Science* 65: 414–432. doi:10.1093/icesjms/fsn048.

Fassbender, A.J. 2014. New approaches to study the marine carbon cycle. PhD dissertation, University of Washington. Proquest, 1/11/2016. *http://hdl.handle.net/1773/27552.*

Fassbender, A.J., C. L. Sabine, and M.F. Cronin. 2016. Net community production and calcification from 7 years of NOAA Station Papa Mooring measurements. *Global Biogeochemical Cycles* 30: 250–267. doi:10.1002/2015GB005205.

Fassbender, A.J., C. L. Sabine, and K. M Feifel. 2016. Consideration of coastal carbonate chemistry in understanding biological calcification. *Geophysical Research Letters*: 1–10. doi:10.1002/2016GL068860.

Fassbender, A.J., C. L. Sabine, N. Lawrence-Slavas, E. H. De Carlo, C. Meinig, and S. Maenner-Jones. 2015. Robust Sensor for Extended Autonomous Measurements of Surface Ocean Dissolved Inorganic Carbon. *Environmental Science & Technology* 49: 3628–3635. doi:10.1021/es5047183.

Feely, R.A., S.R. Alin, B. Hales, G. Johnson, L. Juranek, R.H. Byrne, W. Peterson, M. Goni, X. Liu, and D. Greeley. 2014. Carbon dioxide, hydrographic and chemical measurements onboard R/V Wecoma during the NOAA PMEL West Coast Ocean Acidification Cruise WCOA2011 (August 12 - 30, 2011). *Carbon Dioxide Information Analysis Center, Oak Ridge National Laboratory, US Department of Energy, Oak Ridge, Tennessee*. doi:10.3334/CDIAC/OTG.COAST_WCOA2011.

Feely, R.A., S.R. Alin, B. Hales, G. Johnson, L. Juranek, R.H. Byrne, W. Peterson, and D. Greeley. 2014. Carbon dioxide, hydrographic and chemical measurements onboard R/V Bell M. Shimada during the NOAA PMEL West Coast Ocean Acidification Cruise WCOA2012 (September 4 - 17, 2012). *Carbon Dioxide Information Analysis Center, Oak*

Ridge National Laboratory, US Department of Energy, Oak Ridge, Tennessee. doi:10.3334/CDIAC/OTG.COAST_WCOA2012.

Feely, R.A., S.R. Alin, B. Hales, G.C. Johnson, R.H. Byrne, W.T. Peterson, X. Liu, and D. Greeley. 2015. Chemical and hydrographic profile measurements during the West Coast Ocean Acidification Cruise WCOA2013 (August 3-29, 2013). *Carbon Dioxide Information Analysis Center, Oak Ridge National Laboratory, US Department of Energy, Oak Ridge, Tennessee*. doi:10.3334/CDIAC/OTG.COAST_WCOA2013.

Feely, R.A., S.R. Alin, J.A. Newton, C. L. Sabine, M. Warner, A. Devol, C. Krembs, and C. Maloy. 2010. The combined effects of ocean acidification, mixing, and respiration on pH and carbonate saturation in an urbanized estuary. *Estuarine, Coastal and Shelf Science* 88: 442–449. doi:10.1016/j.ecss.2010.05.004.

Feely, R.A., and C. L. Sabine. 2011. Carbon dioxide and hydrographic measurements during the 2007 NACP West Coast Cruise. *Carbon Dioxide Information Analysis Center, Oak Ridge National Laboratory, US Department of Energy, Oak Ridge, Tennessee*. doi:10.3334/CDIAC/otg.CLIVAR_NACP_West_Coast_Cruise_2007.

Feely, R.A., C. L. Sabine, J. M. Hernandez-Ayon, D. Ianson, and B. Hales. 2008. Evidence for Upwelling of Corrosive "Acidified" Water onto the Continental Shelf. *Science* 320: 1490–1492. doi:10.1126/science.1155676.

Feely, R.A., C. L. Sabine, K. Lee, W. Berelson, J.A. Kleypas, V. J. Fabry, and F. J. Millero. 2004. Impact of Anthropogenic CO_2 on the $CaCO_3$ System in the Oceans. *Science* 305: 362–366. doi:10.1126/science.1097329.

Feely, R.A., R. Wanninkhof, H. B. Milburn, C. E. Cosca, M. Stapp, and P. P. Murphy. 1998. A new automated underway system for making high precision pCO_2 measurements onboard research ships. *Analytica Chimica Acta* 377: 185–191. doi:10.1016/S0003-2670(98)00388-2.

Friis, K, A. Kortzinger, and D.W.R. Wallace. 2003. The salinity normalization of marine inorganic carbon chemistry data. *Geophysical Research Letters*. doi:10.1029/2002GL015898.

Fry, C. H., T. Tyrrell, M. P. Hain, N.R. Bates, and E. P. Achterberg. 2015. Analysis of global surface ocean alkalinity to determine controlling processes. *Marine Chemistry* 174. Elsevier B.V.: 46–57. doi:10.1016/j.marchem.2015.05.003.

Gray, S.E.C., M.D. DeGrandpre, T. S. Moore, T.R. Martz, G. Friederich, and K. S. Johnson. 2011. Applications of in situ pH measurements for inorganic carbon calculations. *Marine Chemistry* 125. Elsevier B.V.: 82–90. doi:10.1016/j.marchem.2011.02.005.

Hernandez-Ayon, J. M., A. Zirino, A.G. Dickson, T. Camiro-Vargas, and E. Valenzuela. 2007. Estimating the contribution of organic bases from microalgae to the titration alkalinity in coastal seawaters. *Limnology and Oceanography: Methods* 5: 225–232. doi:10.4319/lom.2007.5.225.

van Heuven, S., D. Pierrot, J W B Rae, E. Lewis, and D.W.R. Wallace. 2011. MATLAB Program Developed for CO_2 System Calculations. ORNL/CDIAC-105b. *ORNL/CDIAC-105b. Carbon Dioxide Information Analysis Center, Oak Ridge National Laboratory, U.S.*

738 *Department of Energy, Oak Ridge, Tennessee*.
739 doi:10.3334/CDIAC/otg.CO2SYS_MATLAB_v1.1.

740 Hickey, B., S. Geier, N. Kachel, and A. MacFadyen. 2005. A bi-directional river plume: The
741 Columbia in summer. *Continental Shelf Research* 25: 1631–1656.
742 doi:10.1016/j.csr.2005.04.010.

743 Hickey, B. M., and N.S. Banas. 2008. Why is the Northern End of the California Current System
744 So Productive? *Oceanography* 21: 90–107.

745 Hofmann, G.E., J. E Smith, K. S Johnson, U Send, L. A. Levin, F. Micheli, A. Paytan, et al.
746 2011. High-frequency dynamics of ocean pH: A multi-ecosystem comparison. *PLoS ONE*
747 6: e28983. doi:10.1371/journal.pone.0028983.

748 Hu, Xinping, Jennifer Beseres Pollack, Melissa R Mccutcheon, Paul A Montagna, and
749 Zhangxian Ouyang. 2015. Long-Term Alkalinity Decrease and Acidification of Estuaries in
750 Northwestern Gulf of Mexico. *Environmental Science & Technology* 49: 3401–3409.
751 doi:10.1021/es505945p.

752 Hunt, C. W., J E Salisbury, and D. Vandemark. 2011. Contribution of non-carbonate anions to
753 total alkalinity and overestimation of pCO_2 in New England and New Brunswick rivers.
754 *Biogeosciences* 8: 3069–3076. doi:10.5194/bg-8-3069-2011.

755 Juranek, L. W., R.A. Feely, D. Gilbert, H. J. Freeland, and L.A. Miller. 2011. Real-time
756 estimation of pH and aragonite saturation state from Argo profiling floats: Prospects for an
757 autonomous carbon observing strategy. *Geophysical Research Letters* 38: n/a–n/a.
758 doi:10.1029/2011GL048580.

759 Kelly, R. P., M. M. Foley, W. S. Fisher, R.A. Feely, B. S. Halpern, G. G. Waldbusser, and M. R.
760 Caldwell. 2011. Mitigating Local Causes of Ocean Acidification with Existing Laws.
761 *Science* 332: 1036–1037. doi:10.1126/science.1203815.

762 Kim, Hyun-Cheol, K. Lee, and Wonyong Choi. 2006. Contribution of phytoplankton and
763 bacterial cells to the measured alkalinity of seawater. *Limnology and Oceanography* 51:
764 331–338. doi:10.4319/lo.2006.51.1.0331.

765 Kuliński, K., B. Schneider, K. Hammer, U. Machulik, and D. Schulz-Bull. 2014. The influence
766 of dissolved organic matter on the acid-base system of the Baltic Sea. *Journal of Marine*
767 *Systems* 132: 106–115. doi:10.1016/j.jmarsys.2014.01.011.

768 Lauvset, S. K., N. Gruber, P. Landschützer, A. Olsen, and J. Tjiputra. 2015. Trends and drivers
769 in global surface ocean pH over the past 3 decades. *Biogeosciences* 12: 1285–1298.
770 doi:10.5194/bg-12-1285-2015.

771 Lee, K., L T. Tong, F. J. Millero, C. L. Sabine, A.G. Dickson, C. Goyet, G. H. Park, R.
772 Wanninkhof, R.A. Feely, and R. M. Key. 2006. Global relationships of total alkalinity with
773 salinity and temperature in surface waters of the world's oceans. *Geophysical Research*
774 *Letters* 33: L19605. doi:10.1029/2006GL027207.

775 Lewis, E., and D.W.R. Wallace. 1998. MATLAB Program Developed for CO_2 System
776 Calculations. ORNL/CDIAC-105. *Carbon Dioxide Information Analysis Center, Oak Ridge*
777 *National Laboratory, U.S. Department of Energy, Oak Ridge, Tennessee*.

778 Liu, X., M. C. Patsavas, and R.H. Byrne. 2011. Purification and characterization of meta-cresol
779 purple for spectrophotometric seawater pH measurements. *Environmental science &*
780 *technology* 45: 4862–8. doi:10.1021/es200665d.

781 Lueker, T.J., A.G. Dickson, and C.D. Keeling. 2000. Ocean pCO_2 calculated from dissolved
782 inorganic carbon, alkalinity, and equations for K_1 and K_2: validation based on laboratory
783 measurements of CO_2 in gas and seawater at equilibrium. *Marine Chemistry* 70: 105–119.
784 doi:10.1016/S0304-4203(00)00022-0.

785 Martz, T., K. Daly, R.H. Byrne, J. Stillman, and D. Turk. 2015. Technology for Ocean
786 Acidification Research: Needs and Availability. *Oceanography* 25: 40–47.
787 doi:10.5670/oceanog.2015.30.

788 McLaughlin, K., S. B. Weisberg, A.G. Dickson, G.E. Hofmann, J.A. Newton, D. Aseltine-
789 Neilson, A. Barton, et al. 2015. Core Principles of the California Current Acidification
790 Network: Linking Chemistry, Physics, and Ecological Effects. *Oceanography* 25: 160–169.
791 doi:10.5670/oceanog.2015.39.

792 Millero, F. J. 2007. The marine inorganic carbon cycle. *Chemical Reviews* 107: 308–341.
793 doi:10.1021/cr0503557.

794 Mucci, A. 1983. The solubility of calcite and aragonite in seawater at various salinities,
795 temperatures, and one atmosphere total pressure. *American Journal of Science* 283: 780–
796 799. doi:10.2475/ajs.283.7.780.

797 Muller, François L.L., and Bjørn Bleie. 2008. Estimating the organic acid contribution to coastal
798 seawater alkalinity by potentiometric titrations in a closed cell. *Analytica Chimica Acta* 619:
799 183–191. doi:10.1016/j.aca.2008.05.018.

800 Newton, J.A., R.A. Feely, E.B. Jewett, P. Williamson, and J.T. Mathis. 2014. *Global Ocean*
801 *Acidification Observing Network: Requirements and Governance Plan*.

802 Orr, J. C., V. J. Fabry, O. Aumont, L. Bopp, S. C. Doney, R.A. Feely, A. Gnanadesikan, et al.
803 2005. Anthropogenic ocean acidification over the twenty-first century and its impact on
804 calcifying organisms. *Nature* 437: 681–6. doi:10.1038/nature04095.

805 Pfeil, B., A. Olsen, D. C. E. Bakker, S. Hankin, H. Koyuk, A. Kozyr, J. Malczyk, et al. 2013. A
806 uniform, quality controlled Surface Ocean CO_2 Atlas (SOCAT). *Earth System Science Data*
807 5: 125–143. doi:10.5194/essd-5-125-2013.

808 Pierrot, D., C. Neill, K. Sullivan, R. D. Castle, R. Wanninkhof, Heike Lüger, T. Johannessen, A.
809 Olsen, R.A. Feely, and C. E. Cosca. 2009. Recommendations for autonomous underway
810 pCO_2 measuring systems and data-reduction routines. *Deep-Sea Research Part II: Topical*
811 *Studies in Oceanography* 56: 512–522. doi:10.1016/j.dsr2.2008.12.005.

812 Raymond, P. A, and J. J Cole. 2003. Increase in the Export of Alkalinity from North America's
813 Largest River. *Science* 301.

814 Raymond, P. A, N.-H. Oh, R E. Turner, and W. Broussard. 2008. Anthropogenically enhanced
815 fluxes of water and carbon from the Mississippi River. *Nature* 451: 449–452.
816 doi:10.1038/nature06505.

817 Rhein, M., S.R. Rintoul, S. Aoki, E. Campos, D. Chambers, R.A. Feely, S. Gulev, et al. 2013.

Observations: Ocean. In *Climate Change 2013: The Physical Science Basis. Contribution of Working Group I to the Fifth Assessment Report of the Intergovernmental Panel on Climate Change*, ed. T. F. Stocker, D. Qin, G. K. Plattner, M. Tignor, S. K. Allen, J. Boschung, A. Nauels, Y. Xia, V. Bex, and P. M. Midgley. Cambridge University Press, Cambridge/New York.

Sabine, C. L., and H.W. Ducklow. 2010. International carbon coordination: Roger Revelle's legacy in the Intergovernmental Oceanographic Commission 23: 48–61.

Sabine, C. L., S. Hankin, H. Koyuk, D. C. E. Bakker, B. Pfeil, A. Olsen, N. Metzl, et al. 2013. Surface Ocean CO_2 Atlas (SOCAT) gridded data products. *Earth System Science Data* 5: 145–153. doi:10.5194/essd-5-145-2013.

Sutton, A. J., R.A. Feely, C. L. Sabine, M.J. McPhaden, T. Takahashi, F. P. Chavez, G. Friederich, and J.T. Mathis. 2014. Natural variability and anthropogenic change in equatorial Pacific surface ocean pCO_2 and pH. *Global Biogeochemical Cycles* 28: 131–145. doi:10.1002/2013GB004679.

Sutton, A. J., C. L. Sabine, R.A. Feely, W.-J. Cai, M.F. Cronin, Michael J. McPhaden, Julio M. Morell, et al. 2016. Using present-day observations to detect when anthropogenic change forces surface ocean carbonate chemistry outside pre-industrial bounds. *Biogeosciences Discussions*: 1–30. doi:10.5194/bg-2016-104.

Sutton, A. J., C. L. Sabine, S. Maenner-Jones, N. Lawrence-Slavas, C. Meinig, R.A. Feely, J.T. Mathis, et al. 2014. A high-frequency atmospheric and seawater pCO_2 data set from 14 open ocean sites using a moored autonomous system. *Earth System Science Data* 6: 353–366. doi:10.5194/essdd-7-385-2014.

Sutton, A. J., C. L. Sabine, S. Maenner-Jones, S. Musielewicz, R. Bott, and J. Osborne. 2011. High-resolution ocean and atmosphere pCO_2 time-series measurements from mooring LaPush_125W_48N. *Carbon Dioxide Information Analysis Center, Oak Ridge National Laboratory, US Department of Energy, Oak Ridge, Tennessee.* doi:0.3334/CDIAC/otg.TSM_LaPush_125W_48N.

Takahashi, T., S. C. Sutherland, D. W. Chipman, J. G. Goddard, and C. Ho. 2014. Climatological distributions of pH, pCO_2, total CO_2, alkalinity, and $CaCO_3$ saturation in the global surface ocean, and temporal changes at selected locations. *Marine Chemistry* 164: 95–125. doi:10.1016/j.marchem.2014.06.004.

Takeshita, Y., C. A. Frieder, T. R. Martz, J. R. Ballard, R.A. Feely, S. Kram, S. Nam, M. O. Navarro, N. N. Price, and J. E. Smith. 2015. Including high-frequency variability in coastal ocean acidification projections. *Biogeosciences* 12: 5853–5870. doi:10.5194/bg-12-5853-2015.

Uppstrom, L.R. 1974. The boron-chlorinity ratio of deep seawater from the Pacific Ocean. *Deep-Sea Research Part I* 21: 161–162.

Waldbusser, G. G., B. Hales, C. J. Langdon, B. A. Haley, P. Schrader, E. L. Brunner, M. W. Gray, C. A. Miller, and I. Gimenez. 2014. Saturation-state sensitivity of marine bivalve larvae to ocean acidification. *Nature Climate Change* 5: 273–280. doi:10.1038/nclimate2479.

Waldbusser, G. G., and J. E. Salisbury. 2014. Ocean acidification in the coastal zone from an organism's perspective: multiple system parameters, frequency domains, and habitats. *Annual review of marine science* 6: 221–47. doi:10.1146/annurev-marine-121211-172238.

Wolf-Gladrow, D. A., R. E. Zeebe, C Klaas, A. Kortzinger, and A.G. Dickson. 2007. Total alkalinity: The explicit conservative expression and its application to biogeochemical processes. *Marine Chemistry* 106: 287–300. doi:10.1016/j.marchem.2007.01.006.

Wootton, T. J., and C. A. Pfister. 2012. Carbon System Measurements and Potential Climatic Drivers at a Site of Rapidly Declining Ocean pH. Edited by Wei-Chun Chin. *PLoS ONE* 7: e53396. doi:10.1371/journal.pone.0053396.

Xue, L., W.-J. Cai, X. Hu, C. L. Sabine, S. Jones, A. J. Sutton, L.-Q. Jiang, and J. J. Reimer. 2016. Sea surface carbon dioxide at the Georgia time series site (2006–2007): Air–sea flux and controlling processes. *Progress in Oceanography* 140. Elsevier Ltd: 14–26. doi:10.1016/j.pocean.2015.09.008.

Yang, Bo, R.H. Byrne, and Michael Lindemuth. 2015. Contributions of organic alkalinity to total alkalinity in coastal waters: A spectrophotometric approach. *Marine Chemistry* 176. Elsevier B.V.: 199–207. doi:10.1016/j.marchem.2015.09.008.

Tables:

Table 1. Cruise names, dates, and number of observations (#Obs.) used in this analysis.

Cruise Name	WA Sampling Dates	#Obs
NOAA WCOA	May 2007	18
UW PRISM	February 2008	150
UW PRISM/EPA	August 2008	154
PacOOS	August 2009	23
UW PRISM	September 2009	146
PacOOS	May 2010	26
PacOOS	August 2010	43
UW PRISM	November 2010	72
UW/Chá bă	May 2011	2
UW/Chá bă	August 2011	1
NOAA WCOA	August 2011	64
UW PRISM	October 2011	112
UW/NANOOS	May 2012	9
NOAA WCOA	September 2012	93
UW/Chá bă	January 2013	4
UW/NANOOS	April 2013	31
NOAA WCOA	August 2013	61
UW/NANOOS	September 2013	37
UW/NSF/SFSU	June 2014	11
WOAC	July 2014	136

Cruise details:

UW/Chá bă: cruises from Seattle to Chá bă mooring
UW/NANOOS: cruises from Seattle to Chá bă mooring with stations in between
UW/PRISM: Puget Sound cruises
UW/PRISM/EPA: Puget Sound and Strait of Juan de Fuca cruise
WOAC: Puget Sound cruise
UW/NSF/SFSU: UW assisted, National Science Foundation supported, San Francisco State University cruise

Table 2. Distribution of samples used in this analysis by geographic region and by month.

	Jan	Feb	Mar	Apr	May	June	July	Aug	Sept	Oct	Nov	Dec	Sum
Outer Coast	4	0	0	15	53	4	0	205	93	9	0	0	**383**
South Sound	0	17	0	0	0	0	16	12	0	21	0	0	**66**
Hood Canal	0	43	0	0	0	0	48	34	4	95	45	0	**269**
Juan de Fuca	0	24	0	16	2	5	12	39	10	40	12	0	**160**
Whidbey Basin	0	13	0	0	0	0	12	13	12	0	0	0	**50**
Central Sound	0	53	0	0	0	2	48	43	65	39	15	0	**265**
Sum	**4**	**150**	**0**	**31**	**55**	**11**	**136**	**346**	**184**	**204**	**72**	**0**	**1193**

Table 3. Empirical TA relationships near Washington State where N is the number of observations used to define the relationship, SR is the salinity range of those observations, 1σ is the residual of the regional fit, and Ref. designates the corresponding reference listed below the table. These relationships were tested against the 1,193 discrete TA bottle samples collected in Washington from the top 25 m of water (**Figure 1**). The resulting mean offsets (Δ) and standard deviations (1σ) are given.

Regression Relationship	N	SR	1σ	Region	Ref.	Δ	1σ
TA = 47.7(±0.2) × **S** + 647(±6)	1,193	20–35	17	WA	AF	-1	17
TA = 50.8 × **S** + 543.5	~24,000	-	20	Central CA	CG	-8	18
TA = 2305 + 53.23×(**S**-35) + 1.85×(**S**-35)^2 - 14.72×(**T**-20) - 0.158×(**T**-20)^2 + 0.062×(**T**-20)×(**Lon**)	258	31–35	8.7	North Pacific	KL	-8	30
TA = 40.49 × **S** + 894.17	36	27–35	-	WA	TW	28	20

S = salinity, **T** = temperature, **Lon** = Longitude.
AF: This study.
CG: (Gray et al. 2011)
KL: (Lee et al. 2006):
TW: (Wootton and Pfister 2012)

Figures:

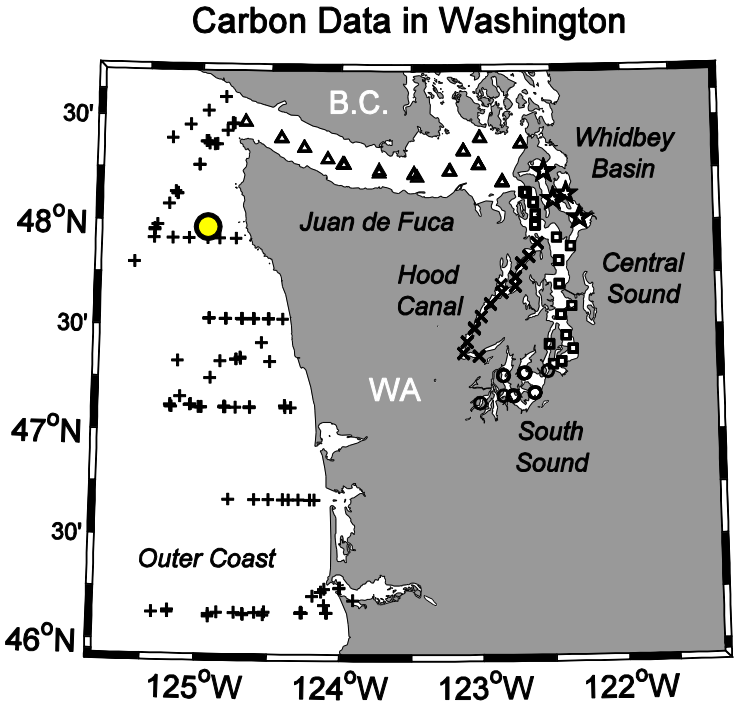

Figure 1. Sample stations where high-quality, dual-parameter carbon data were collected near Washington State during coastal survey cruises. Symbols signify the six geographical regions samples were collected from, including: Hood Canal, South Sound, Central Sound, Whidbey Basin, Strait of Juan de Fuca, and the Outer Coast. The location of the NANOOS-OAP Chá bă surface mooring is also shown with a yellow circle.

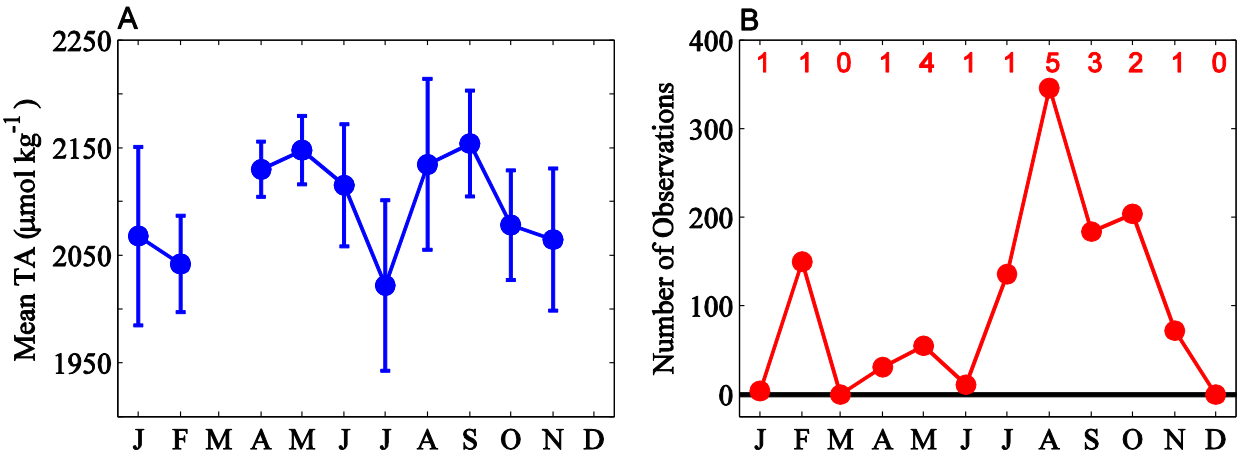

Figure 2. (**A**) Mean TA (± 1σ) and (**B**) the total number of observations per month for samples collected within the top 25 m of water at the stations shown in Figure 1. The number of unique years in which samples were collected for each month is shown at the top of the plot.

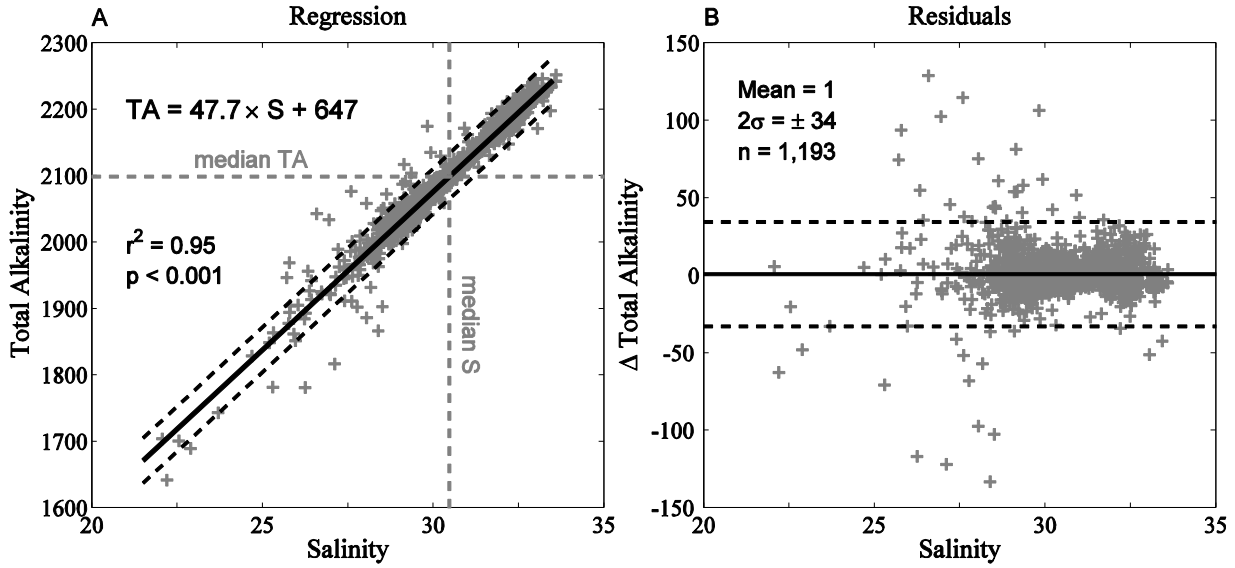

Figure 3. (**A**) Linear-least-squares regression of TA and salinity using samples collected from the top 25 m of water at stations shown in Figure 1. Dashed lines show the 95% confidence limits (±2σ). (**B**) Residuals of the empirical regression fit versus salinity.

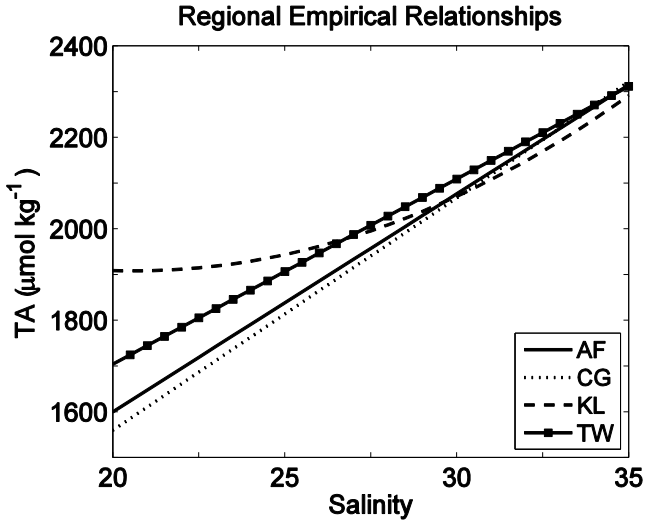

Figure 4. Regional empirical TA-salinity relationship curves in the salinity range of 20–35 using a temperature of 11 °C (average temperature of calibration dataset) and longitude of 125 °W for the KL fit. References and equations for the different curves are given in **Table 3**.

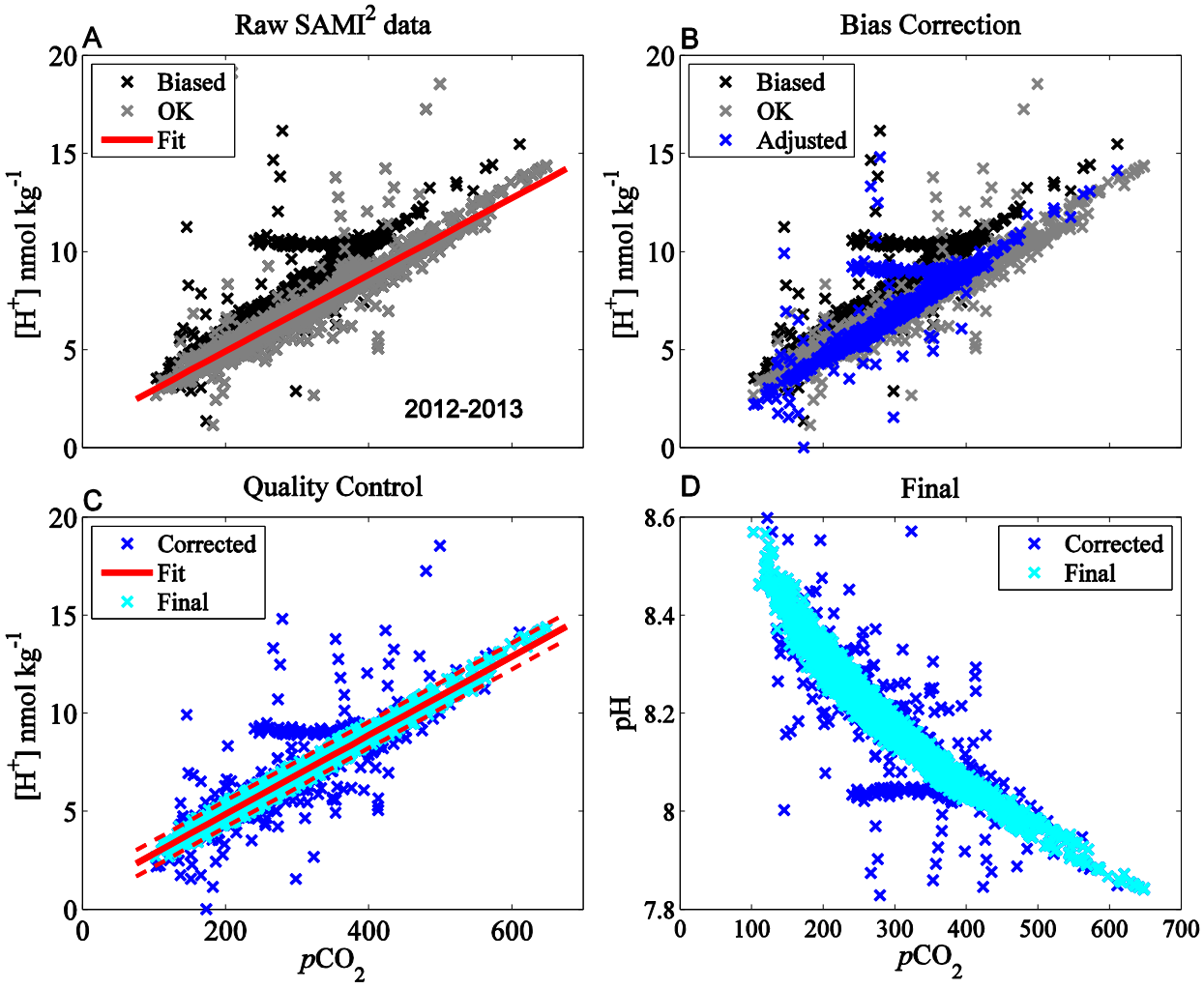

Figure 5. (**A**) Raw SAMI^2 pH data converted to total scale hydrogen ion concentration ([H^+]) in units of nmol kg^{-1} from the NANOOS-OAP Chá bă mooring (n=6,467). Values from the 2012–2013 deployment are highlighted in black to display the measurement bias. A fit to the unbiased data is shown in red. (**B**) Same as (**A**) without the fit line and showing the adjusted data. (**C**) Corrected [H^+] with final fit ($[H^+] = 0.0201 \times (pCO_2) + 0.8606$) and ±3σ window shown in red. Data outside of the ±3σ window (n=275, ~4% of data) are considered outliers and are excluded from the analysis. The final [H^+] dataset is plotted in cyan. (**C**) Corrected and final data shown in pH space.

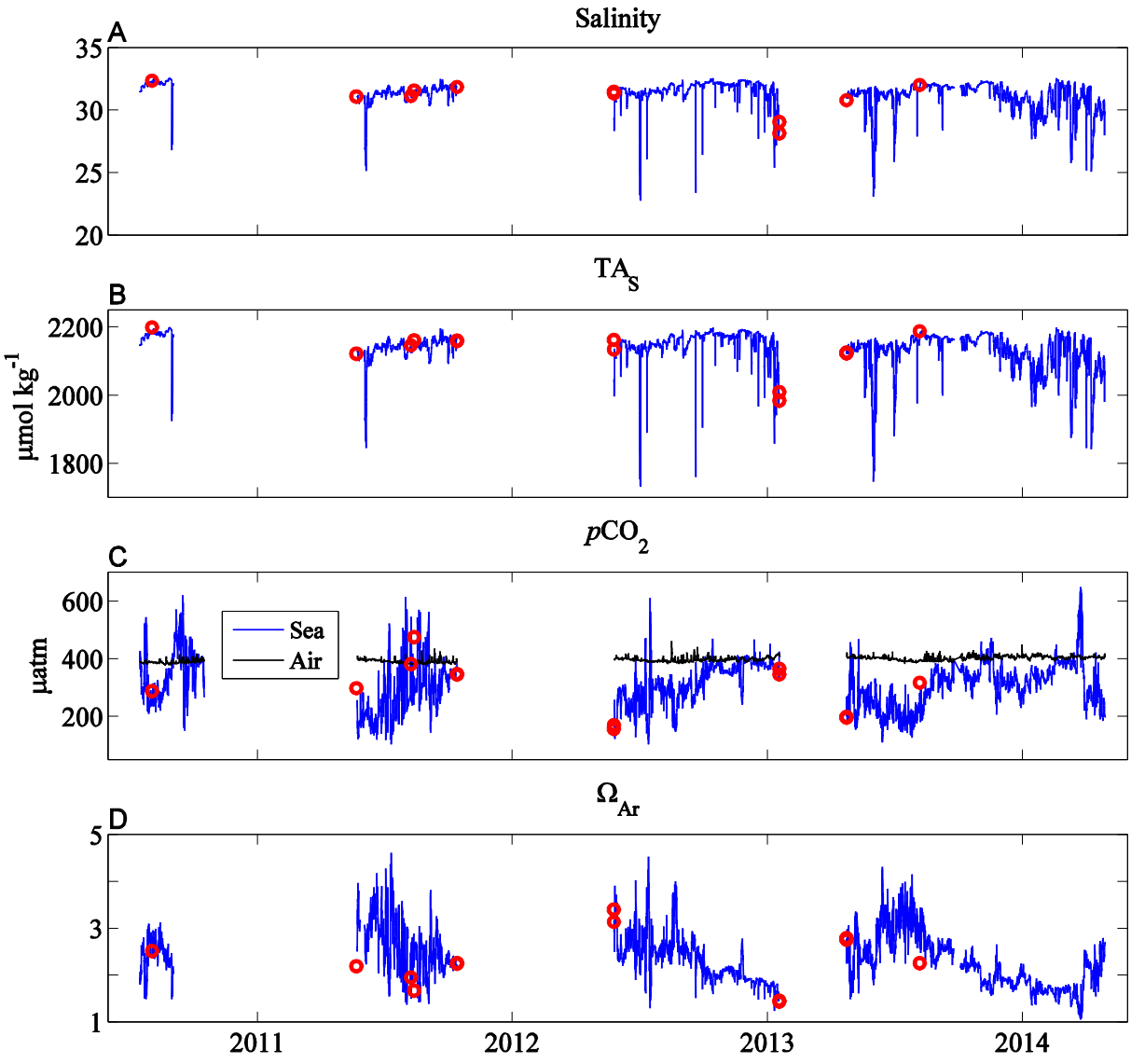

Figure 6. Chá bă mooring (**A**) salinity, (**B**) Total Alkalinity estimated from salinity (TA_S), (**C**) atmospheric boundary layer and sea surface pCO_2, and (**D**) Ω_{Ar}. Red circles in each plot are from discrete bottle samples collected within the top 5 m of water at stations near the mooring. In subplots **C** and **D** the discrete values were calculated from measurements of DIC and TA.

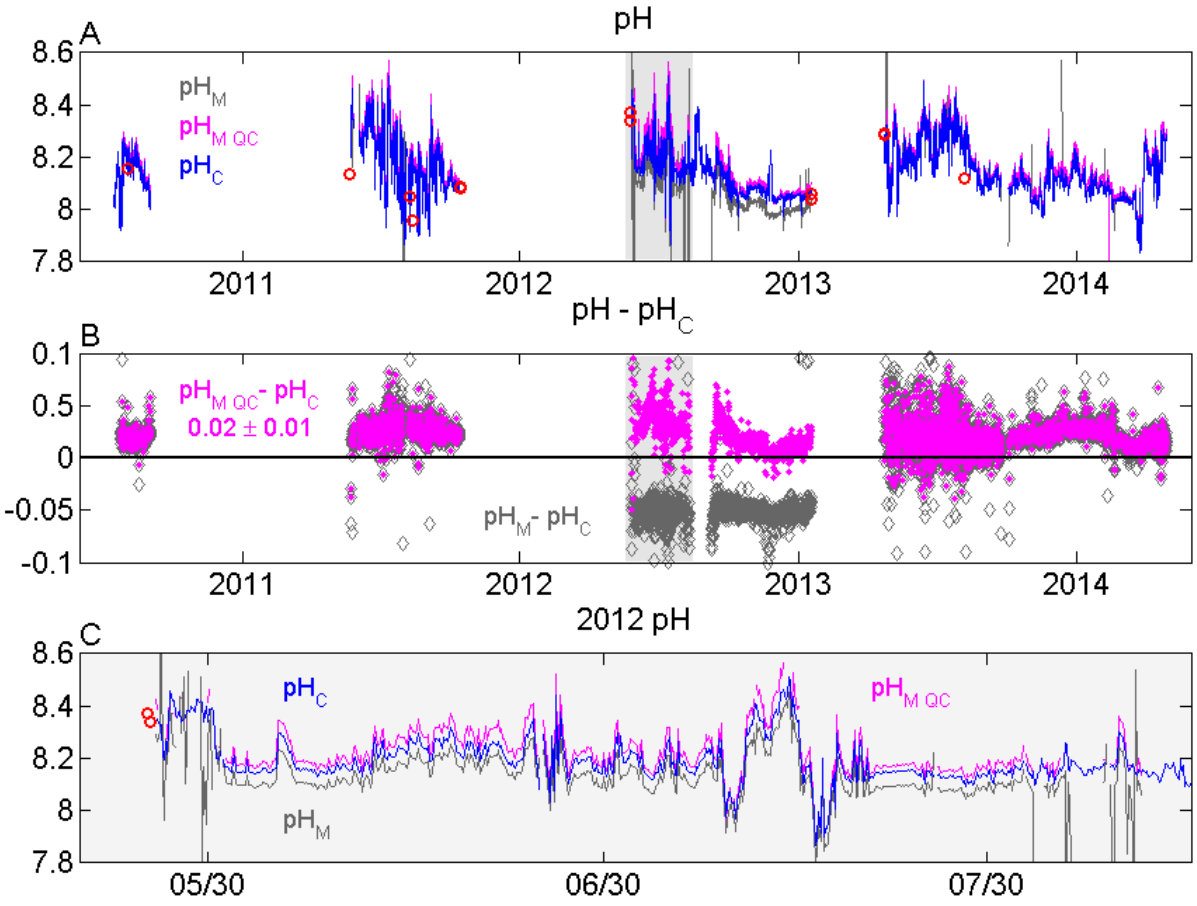

Figure 7. (**A**) Measured pH values, before (pH_M) and after quality control ($pH_{M\ QC}$), as well as calculated pH values (pH_C). (**B**) The difference between measured and calculated pH values before and after quality control. The mean difference and ±1σ is given for $pH_{M\ QC}$ - pH_C. Gray shading in **A** and **B** highlights the data shown in **C** for the summer 2012 Chá bă mooring deployment. Red circles in **A** and **C** were calculated from discrete measurements of DIC and TA collected within the top 5 m of water at stations near the mooring.

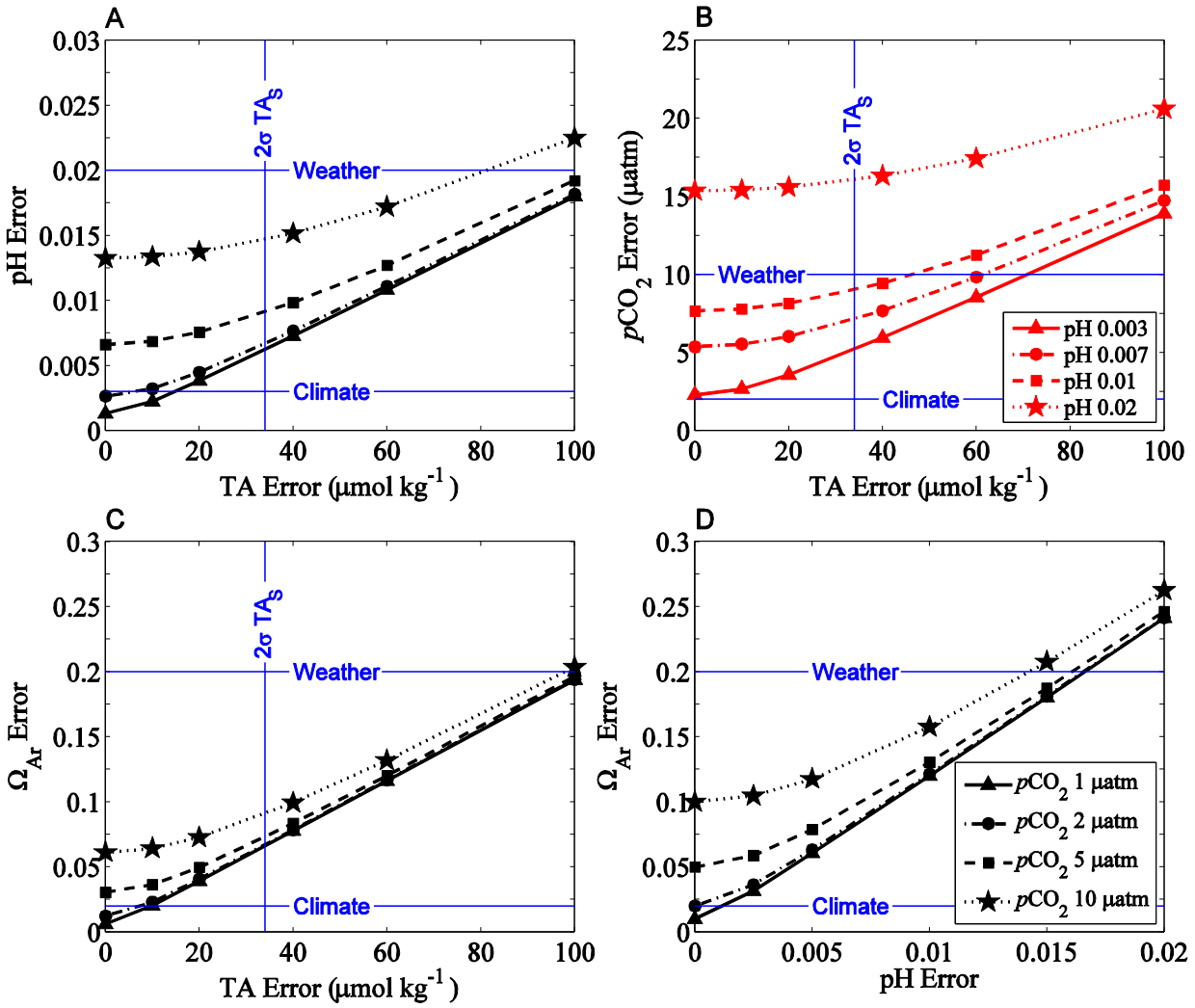

Figure 8. Calculation sensitivities of (**A**) pH (**B**) pCO_2 and (**C**-**D**) aragonite saturation state (Ω_{Ar}) to errors in estimated TA (TA_S) and *in situ* pH and pCO_2. Hypothetical input errors for TA_S, pH, and pCO_2 are shown on the x-axes and in the legends. The legend in **D** also applies to **A** and **C**. Horizontal blue lines display the C-CAN and GOA-ON "weather" and "climate" data-quality objectives. These objectives are defined as uncertainties of 2.5% and 0.5% for pCO_2, and 10% and 1% for Ω_{Ar}, respectively. Values of 400 µatm for pCO_2 and 2 for Ω_{Ar} were used to compute the percentile objectives. Vertical blue lines indicate the 95% confidence limit (2σ TA_S) for the WA TA-S relationship.